The EMBO Journal (2005) 24, 473–486 | © 2005 European Molecular Biology Organization | All Rights Reserved 0261-4189/05
www.embojournal.org

THE EMBO JOURNAL

Interplay between components of a novel LIM kinase–slingshot phosphatase complex regulates cofilin

Juliana Soosairajah[1,4], Sankar Maiti[2,4], O'Neil Wiggan[2], Patrick Sarmiere[2], Nathalie Moussi[1], Boris Sarcevic[3], Rashmi Sampath[2], James R Bamburg[2,5,*] and Ora Bernard[1,5,*]

[1]The Walter & Eliza Hall Institute of Medical Research, Victoria, Australia, [2]Department of Biochemistry and Molecular Biology, Colorado State University, Fort Collins, CO, USA and [3]Cancer Research Program, Garvan Institute of Medical Research, Darlinghurst, NSW, Australia

Slingshot (SSH) phosphatases and LIM kinases (LIMK) regulate actin dynamics via a reversible phosphorylation (inactivation) of serine 3 in actin-depolymerizing factor (ADF) and cofilin. Here we demonstrate that a multi-protein complex consisting of SSH-1L, LIMK1, actin, and the scaffolding protein, 14-3-3ζ, is involved, along with the kinase, PAK4, in the regulation of ADF/cofilin activity. Endogenous LIMK1 and SSH-1L interact *in vitro* and co-localize *in vivo*, and this interaction results in dephosphorylation and downregulation of LIMK1 activity. We also show that the phosphatase activity of purified SSH-1L is F-actin dependent and is negatively regulated via phosphorylation by PAK4. 14-3-3ζ binds to phosphorylated slingshot, decreases the amount of slingshot that co-sediments with F-actin, but does not alter slingshot activity. Here we define a novel ADF/cofilin phosphoregulatory complex and suggest a new mechanism for the regulation of ADF/cofilin activity in mediating changes to the actin cytoskeleton.

The EMBO Journal (2005) **24,** 473–486. doi:10.1038/sj.emboj.7600543; Published online 20 January 2005
Subject Categories: cell & tissue architecture; signal transduction
Keywords: ADF/cofilin; LIMK1; PAK4; Slingshot; 14-3-3

Introduction

Intrinsic and extrinsic signals regulate the dynamic nature of actin filament formation through an abundance of actin-binding and regulatory molecules. Filament-capping proteins, filament-destabilizing proteins, and monomer sequestering molecules can influence the formation, elongation, and destabilization of actin filaments (Pollard and Borisy, 2003). Regulation of these individual pathways ultimately function to cause changes in the actin cytoskeleton.

Proteins of the actin-depolymerizing factor (ADF)/cofilin (AC) family dynamically regulate the actin network by increasing the off-rate of actin monomers from the pointed end of actin filaments and by filament severing (reviewed in Bamburg and Wiggan, 2002). Phosphorylation of serine 3 (ser 3) by the LIM or TES kinases results in AC inactivation, whereas dephosphorylation by SSH phosphatases results in their reactivation. Critical to our understanding of the integration of signalling pathways regulating actin function is an understanding of the mechanisms influencing AC activity.

The two LIM kinases, LIMK1 and LIMK2, are expressed in most tissues (Ikebe *et al*, 1998; Foletta *et al*, 2004) and negatively regulate the actin-dynamizing activities of AC. LIMK are regulated by the Rho GTPases (Arber *et al*, 1998; Yang *et al*, 1998) that, through their effectors Rho-kinase (ROCK) and p21-activated kinases (PAK1 and 4), activate LIMK1 and 2 by phosphorylation at Thr 508 and 505, respectively (Edwards and Gill, 1999; Maekawa *et al*, 1999; Ohashi *et al*, 2000; Sumi *et al*, 2001). LIMK1 associates with 14-3-3 scaffold proteins (Birkenfeld *et al*, 2003), which could affect its activity, localization, and proximity to other effector molecules (Fu *et al*, 2000). Overexpression of 14-3-3ζ *in vivo* promotes the accumulation of the inactive, phosphorylated form of AC in cells (Gohla and Bokoch, 2002). However, it is unclear whether this involves protection from dephosphorylation or increased phosphorylation.

Reactivation of AC proteins occurs by dephosphorylation (Morgan *et al*, 1993), brought about by a class of phosphatases, named slingshot (SSH) (Niwa *et al*, 2002). SSH phosphatases contain conserved A and B domains with unknown functions, a protein phosphatase domain (PTP) containing the catalytic sequence of HCxxGxxR, and in some family members, a C-terminal F-actin-binding region. Currently, three human and mouse isoforms, SSH-1, 2, and 3, have been identified, each with long and short variants (Niwa *et al*, 2002; Ohta *et al*, 2003). Each member has somewhat different tissue expression patterns and phosphatase activity (Ohta *et al*, 2003), but their regulation remains to be determined.

Here we demonstrate that the regulation of AC activity occurs most likely through dynamic associations between actin, 14-3-3ζ, slingshot, PAK4, and LIMK1. Our results show compartmentalization of SSH-1L and LIMK1, and SSH-1L and 14-3-3ζ in neuronal growth cones and to lamella and ruffles in constitutively active rac1-expressing fibroblasts. We demonstrate that purified hSSH-1L, LIMK1, and 14-3-3ζ interact *in vitro* and that F-actin is required for purified hSSH-1L to dephosphorylate phosphoAC *in vitro*. In addition, hSSH-1L can dephosphorylate active LIMK1 on Thr 508, and it is thus a LIMK1 phosphatase, as well as a pAC phosphatase.

*Corresponding authors. JR Bamburg, Department of Biochemistry and Molecular Biology, Colorado State University, 235 MRB, Fort Collins, CO 80523-1870, USA. Tel.: +1 970 491 6096; Fax: +1 970 491 0494; E-mail: jbamburg@lamar.colostate.edu or O Bernard, Walter and Eliza Hall Medical Research, Parkville 3052, Victoria, Australia. Tel.: +61 39 345 2555; E-mail: bernard@wehi.edu.au
[4]These authors contributed equally to the results presented in this manuscript
[5]Senior authors contributed equally to this work

Received: 12 March 2004; accepted: 10 December 2004; published online: 20 January 2005

Furthermore, phosphorylation of hSSH-1L by PAK4 negatively regulates its activity, providing a reciprocal control of LIMK1 and SSH-1L by PAK4.

Results

SSH-1L can co-localize with LIMK1 and 14-3-3ζ in discrete regions within neuronal and non-neuronal cells

Endogenous LIMK1 is localized to the growth cones of E18 rat hippocampal neurons, regions also enriched in endogenous SSH-1L (Figure 1Aa–d). 14-3-3 is also enriched in growth cones, where it shows substantial overlap to regions of high SSH-1L staining (Figure 1Ba–d). As observed with LIMK1, SSH-1L is not exclusively co-localized with 14-3-3 in these cells. However, these data suggest a potential dynamic and regulated process promoting the association of SSH with other regulators of AC proteins.

In the osteosarcoma cell line, Saos-2, LIMK1 is localized to focal adhesions (Figure 1Cb–c), whereas SSH-1L staining is more diffuse. However, overexpressed hSSH-1L does co-localize with LIMK1 at focal adhesions (Figure 1Cd–f). Saos-2 cells expressing constitutively active rac (racV12) lose focal adhesions and both LIMK1 and SSH-1L associate with a circumferential band of actin in the lamella (Figure 1Cg–i), and are found in membrane ruffles (Figure 1Cj–l). Thus, LIMK1 and SSH-1L localize to the same cellular domains in response to rac signalling.

SSH interacts with several proteins involved in the regulation of actin dynamics

To determine which proteins associate with the different forms of hSSH, we overexpressed His/myc-hSSH (1L, 1S, 2S and 3S) in HEK293 cells, bound, washed, and eluted the hSSH isoforms and their associated proteins from nickel resin at neutral pH (Figure 2A). In addition to the expected SSH isoforms detected on a Western blot, endogenous LIMK1 and 14-3-3 were in all eluates (Figure 2A). Actin was present in all samples except those from cells expressing hSSH-1S, which also had the least 14-3-3 binding. When resin washes were at pH > 8, no endogenous LIMK1 remained associated with any of the bound hSSH isoforms and actin and 14-3-3 remained associated with only the hSSH-1L (Figure 2B), suggesting that it has the highest affinity for these proteins.

Association between endogenous LIMK1 and SSH

Most cell lines examined expressed both LIMK1 and SSH-1L (data not shown). Mouse embryo fibroblasts (MEFs) expressed both proteins at comparable levels and therefore were used to study their association. MEF lysate was incubated with anti-LIMK1 mouse mAb and the immunocomplexes were subjected to Western blot analysis with rabbit anti-SSH-1L antibodies. Association between endogenous LIMK1 and SSH was observed (Figure 3A).

The kinase domain of LIMK1 and the N-terminal A and B and phosphatase domains of hSSH1L are required for their association

To identify the region in the LIMK1 protein responsible for its co-immunoprecipitation with SSH, Flag-tagged LIM, PDZ and kinase domains (F-LIM, F-PDZ, and F-kinase), and myc-tagged hSSH-1L (myc-hSSH-1L), cDNA constructs (see Figure 2C for nomenclature of untagged fragments) were transfected separately into COS-7 cells. After 48 h, the lysates were combined and the myc-tagged proteins immunoprecipitated with anti-myc antibodies. Samples were analysed by Western blotting for Flag. The kinase domain, and not the LIM or PDZ domains, mediates the interaction with SSH-1L (Figure 3B). To identify the region in hSSH-1L responsible for the interaction with LIMK1, extracts of mammalian cells expressing GST-SSH-A + B, the phosphatase domain (GST-Pase), and the C-terminal truncated GST-SSH-t were incubated with extracts of mammalian cells expressing F-LIMK1 (Figure 3C). The GST-fusion proteins were pulled down and subjected to Western blot analysis. F-LIMK1 was associated with GST-SSH-A + B, GST-SSH-Pase, and GST-SSH-t, but not with GST alone. Thus, SSH-1L associates with LIMK1 via its A + B and the phosphatase domains.

The catalytic activities of LIMK1 and SSH are not essential for their interaction

To determine whether the activity of the LIMK1 kinase domain is important for its interaction with slingshot, GFP-tagged full-length and kinase domains of active and inactive LIMK1 and GST-SSH-t were expressed either separately or together in 293T cells. After 48 h, the GST-tagged proteins were pulled down and the protein complexes analysed on Western blots. Both wild-type and kinase-dead LIMK1 bound to GST-SSH-t (Figure 3D) and GST-SSH-t (CS) (data not shown), indicating that active kinase and phosphatase are not necessary for this association.

hSSH-1L directly interacts with the kinase domain of LIMK1

As actin and 14-3-3 proteins associate with SSH-1L (Figure 2), we sought to determine whether LIMK1 and hSSH-1L interact directly. We therefore purified the His/myc-hSSH-1L from overexpressing HEK293 cells. Most hSSH-1L-associated proteins are removed from the nickel resin by washing with 2.5 M urea. The urea was removed and the purified hSSH-1L eluted (Figure 4A). GST-LIMK1 was purified from overexpressing HEK293 cells on glutathione Sepharose and washed to remove contaminating proteins prior to elution. Neither GST-

Figure 1 Localization of LIMK1, hSSH-1L and 14-3-3 in neuronal growth cones and Saos-2 cells. (**A**) Endogenous LIMK1 and endogenous SSH-1L localization in the growth cone of an E18 rat hippocampal neuron. (a) Phase, and epi-fluorescence images of same growth cone labelled with (b) rat anti-LIMK1 and (c) rabbit anti-hSSH-1L (Supplementary Figure 1). (d) Overlay of fluorescence images. Bar in Aa for rows A and B = 5 μm. (**B**) Endogenous SSH-1L and 14-3-3 in the growth cone of an E18 hippocampal neuron. (a) Phase, and epi-fluorescence images of same growth cone labelled with (b) 14-3-3 pan antibody and (c) rabbit anti-hSSH-1L. (d) Overlay of fluorescence images. (**C**) Saos-2 cells immunostained for endogenous (a, g, j) or overexpressed (d) SSH-1L, LIMK1 (b, e, h, k) and an overlay (c) showing little co-localization. (d–f) Saos-2 cells overexpressing hSSH-1L which now co-localizes with LIMK1 at focal adhesion (arrow) (d) as seen in the overlay (f). (g–l) Saos-2 cell expressing the constitutively active V12rac. Overlay in (i) shows co-localization to a cortical band (arrow in h) that contains F-actin (not shown) and to membrane ruffles (arrows in k) seen at a higher focal plane of a different cell (j–l). Bars = 10 μm in a–f and 5 μm in j–l.

LIMK1 nor hSSH-1L contained actin or 14-3-3 (Figure 4A). Purified GST-LIMK1 and His-hSSH-1L were incubated *in vitro*. Purified hSSH-1L was pulled down on glutathione beads only in the presence of GST-LIMK1 and GST-LIMK1 was pulled down on nickel beads only in the presence of His-hSSH-1L (Figure 4B). To demonstrate that the kinase domain mediated

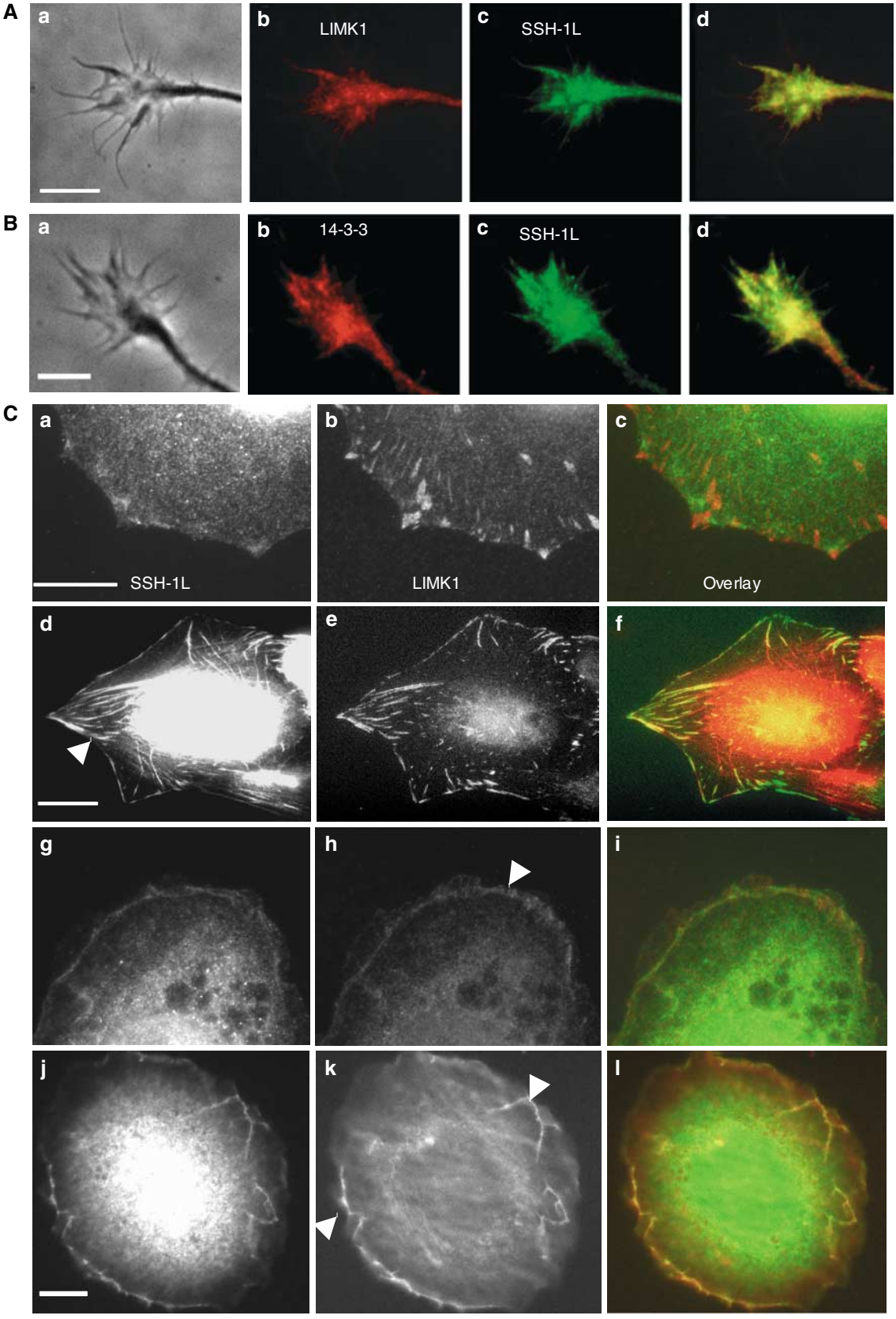

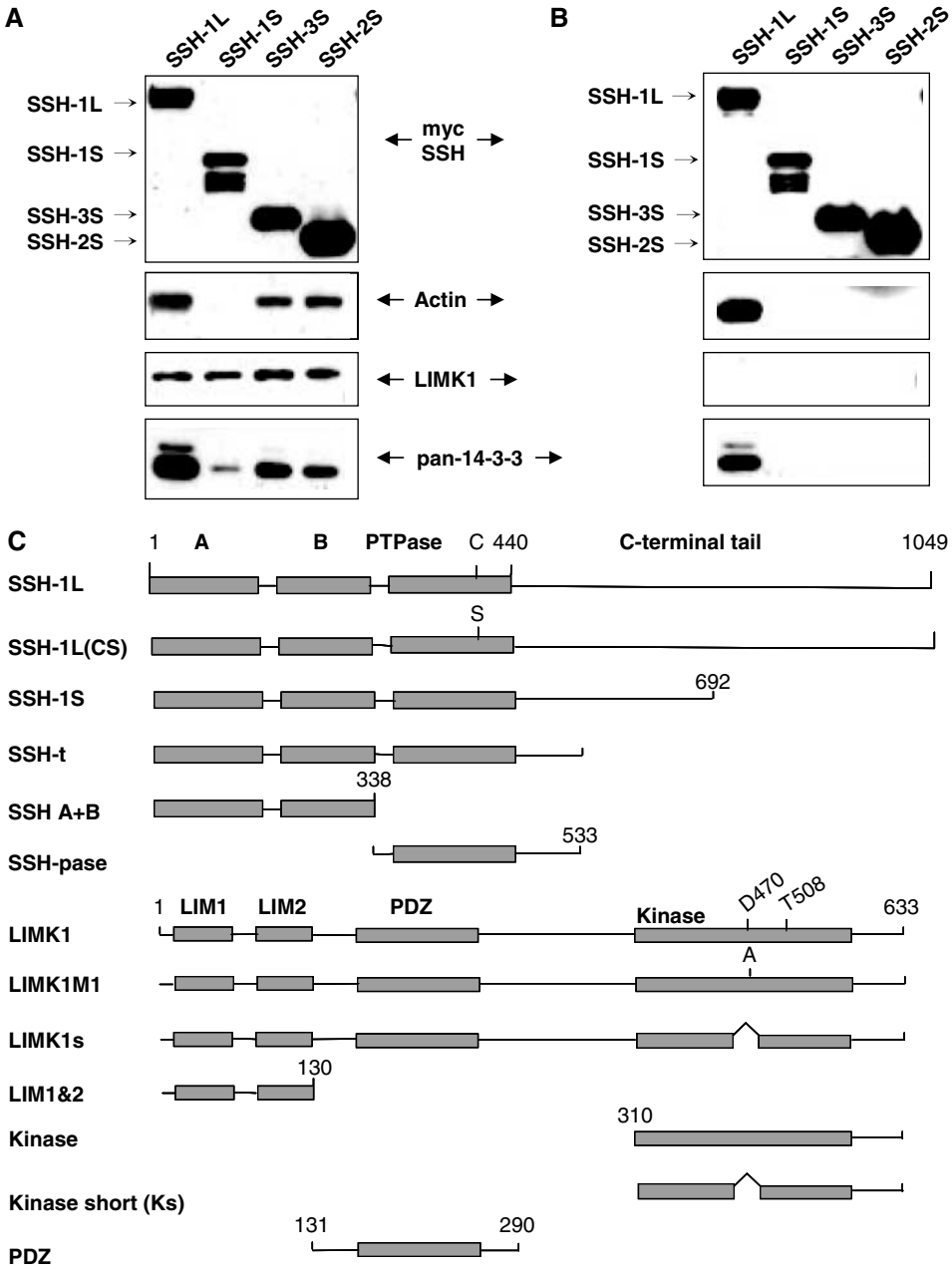

Figure 2 Identification of proteins associated with overexpressed His-myc hSSH-1l, 1S, 2S, and 3S in HEK 293 cells. Lysates from 10 cm dishes of HEK293 cells infected 48 h earlier with adenoviruses expressing His-myc hSSH-1L, 1S, 2S, and 3S were passed over nickel resin, washed with lysis buffer and eluted with lysis buffer containing 250 mM imidazole. (**A**) Immunoblots of proteins eluted at pH < 8. (**B**) Immunoblots of proteins eluted at pH > 8.3. (**C**) Domain organization of SSH-1L and LIMK1, showing the nomenclature of the parental fragments used in this study. Most of these fragments were tagged with His, myc, Flag (F), GST, GFP or HA when used for expression experiments.

this direct binding, the kinase domain of bacterially expressed His-LIMK1 was incubated with bacterially expressed GST-SSH-t (C-terminal deleted) coupled to glutathione Sepharose. The His-kinase domain interacted with GST-hSSH-t but not with GST alone (Figure 4C), suggesting a direct interaction between SSH and the LIMK1 kinase domain. Furthermore, since these domains were bacterially expressed, it is unlikely this interaction requires specific post-translational modifications or is bridged by actin.

Slingshot protein is a LIMK1 phosphatase

The direct interaction between LIMK1 and SSH suggested that some functional co-regulation might be involved. To test if SSH alters LIMK1 activity, we compared the ability of wild-type and phosphatase-inactive SSH-1L (CS; C393S) to dephosphorylate LIMK1 and affect its kinase activity. LIMK1 is activated by phosphorylation of Thr 508, followed by autophosphorylation on serines; therefore, LIMK1 activity positively correlates with its level of phosphorylation.

To demonstrate the direct effect of hSSH-1L on phospho-LIMK1 (p-LIMK1), purified GST-LIMK1, bound to glutathione beads, was autophosphorylated with [γ^{32}P]ATP followed by washing. [^{32}P]GST-LIMK1 was incubated with either active or inactive SSH-1L for 10–100 min. The amount of [^{32}P] released by the phosphatase was measured before proteins were subjected to Western blotting. The amount of [^{32}P] associated

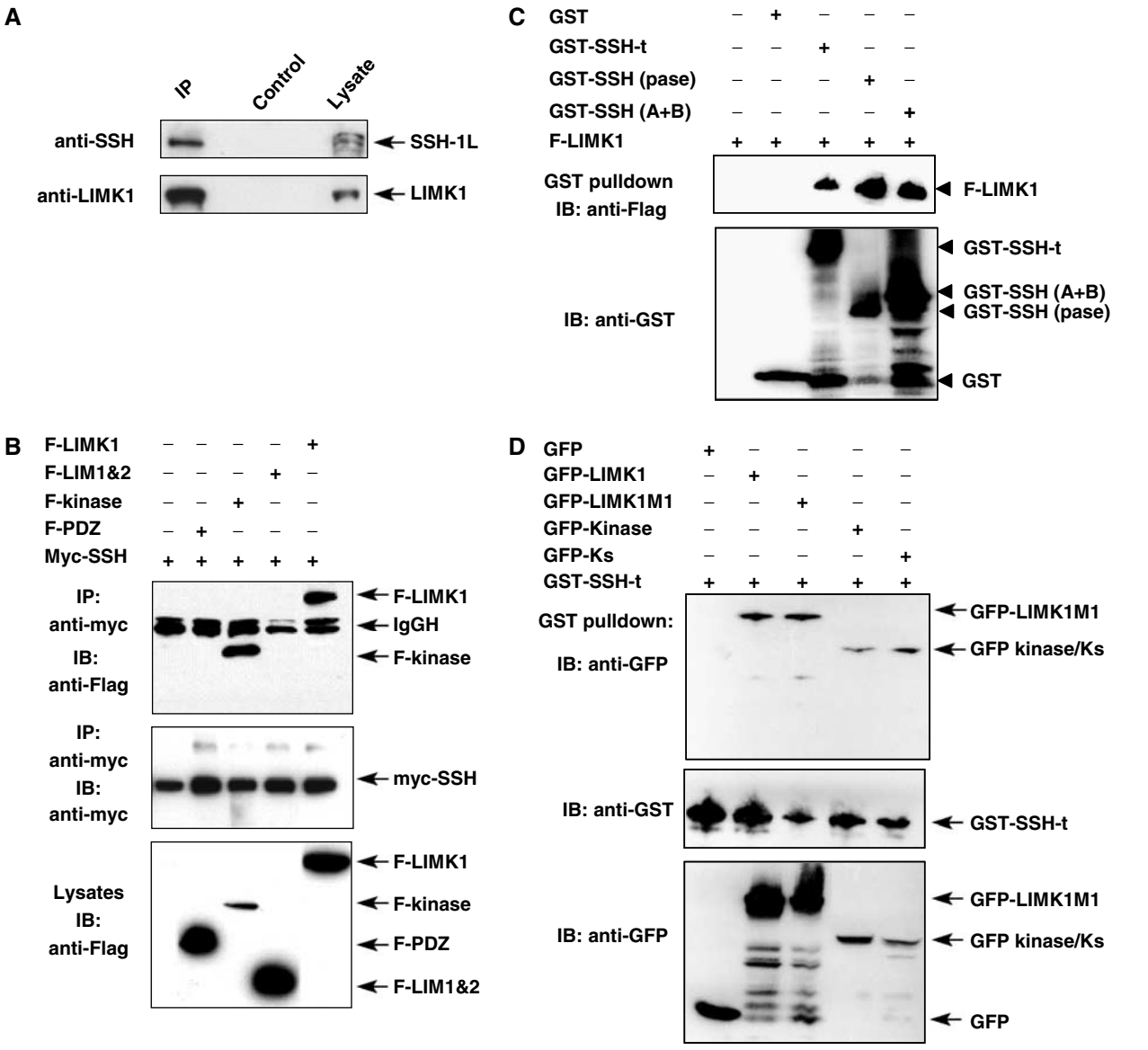

Figure 3 Analysis of LIMK1 and SSH interaction. (**A**) Interaction between endogenous LIMK1 and endogenous SSH-1L. MEF lysates immunoprecipitated with mouse anti-LIMK1 mAb were subjected to Western blotting with anti-SSH antibodies (top panel). The filter was reprobed with rat anti-LIMK1 mAb to show that LIMK1 was present in the IP and in the lysate (bottom panel). As negative control, the lysate was immunoprecipitated with IgG2. (**B**) Flag-tagged full-length (F-LIMK1) and the kinase domain of LIMK1 (F-kinase) but not F-LIM1&2 and F-PDZ domains interact with the full-length myc-SSH-1L. F-kinase bound 10 × more myc-SSH-1L protein than full-length LIMK1. The filter was reprobed with rabbit anti-myc polyclonal antibodies (middle panel) to demonstrate that equal amounts of myc-SSH were immunoprecipitated, whereas the bottom panel shows expression of the different LIMK1 proteins in lysates prepared from transfected COS-7 cells. (**C**) F-LIMK1 interacts with GST-SSH-t, the N-terminal A + B domain, and the phosphatase domain, but not with GST alone. (**D**) GST-SSH-t interacts with GFP-tagged active (GFP-LIMK1) or inactive full-length and kinase domains of LIMK1 but not with GFP alone. GFP-LIMK1M1 represents kinase-dead LIMK1 (D470A), GFP-K is GFP-tagged kinase domain, and GFP-Ks is the GFP-tagged dominant-negative splice variant kinase domain of LIMK1.

with the LIMK1 band was determined from PhosphorImager analysis. All samples were normalized for the amounts of LIMK1 and hSSH-1L, as determined by densitometric analysis of the immunoblotted SSH and LIMK1 proteins. Reduced levels of [^{32}P]LIMK1 and increased levels of free [^{32}P] were observed when p-LIMK1 was incubated in the presence of active SSH-1L. In contrast, in the presence of catalytically inactive SSH-1L (CS), there was no change in either the level of p-LIMK1 or free [^{32}P], further suggesting that LIMK1 is a substrate for SSH-1L phosphatase (Figure 5A).

Similar experiments were performed with C-terminal truncated hSSH-1L (SSH-t, aa 1–533). Affinity-purified [^{32}P]LIMK1 (0.1 μg) was used as substrate for bacterially and mammalian expressed GST-SSH-1L or GST-SSH-1L-t, using expressed GST as a control. In the presence of both mammalian and bacterially expressed GST-SSH-t, the phosphorylation of LIMK1 was greatly reduced, indicating that the C-terminal domain of SSH-1L is not necessary for its phosphatase activity towards LIMK1. In addition, bacterially expressed GST-SSH-t was more active than its mammalian

expressed counterpart (Figure 5B and C). This was not true for the bacterial SSH-1L, because it requires F-actin for activity (see below).

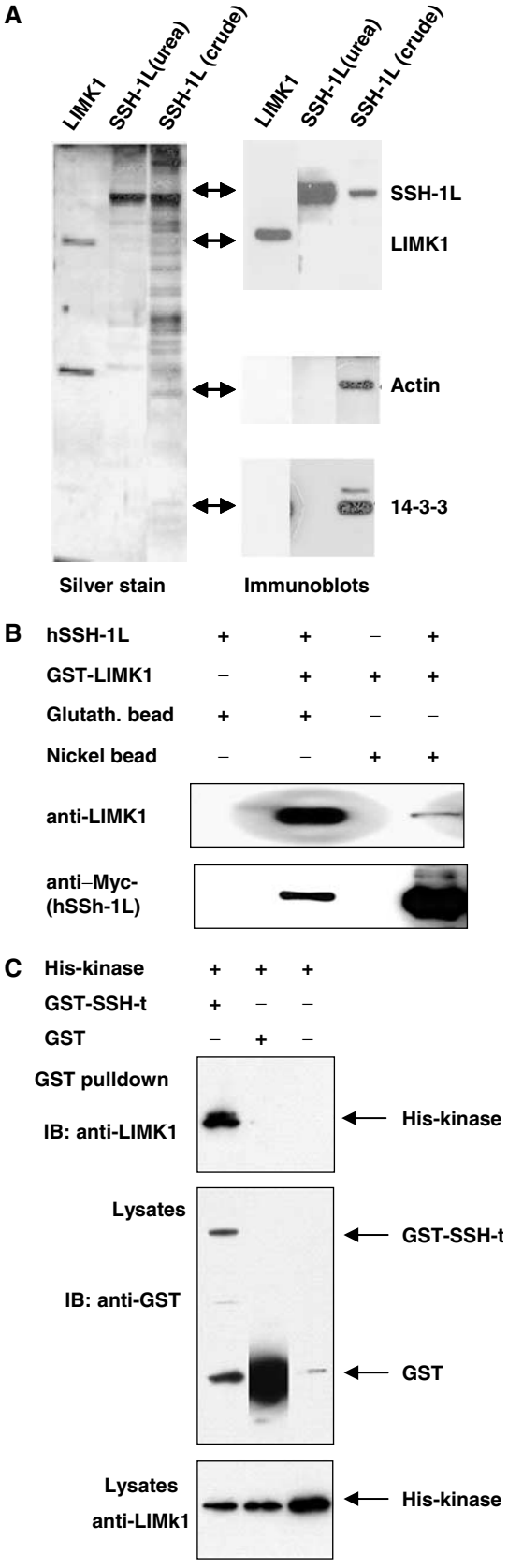

LIMK1 and 2 have high homology and they both interact with SSH (Figure 3 and data not shown). To test whether this interaction leads to the dephosphorylation of LIMK2, lysates from cells expressing HA-LIMK1 and HA-LIMK2 were immunoprecipitated with anti-HA antibodies subjected to the *in vitro* phosphatase assay. In the presence of GST-SSH-t purified from mammalian and bacterial cells, the levels of p-LIMK1 and p-LIMK2 decreased. GST-SSH-t purified from bacteria was much more active than that purified from mammalian cells. Significantly, the level of p-LIMK1 decreased by twice as much as the level of p-LIMK2 when normalized to the amount of LIMK loaded (Figure 5D), suggesting that LIMK1 is a better SSH-1 substrate than LIMK2.

Slingshot downregulates the activity of LIMK1 towards cofilin

To identify the phosphoamino acids of LIMK1 dephosphorylated by SSH, we first tested the ability of SSH to dephosphorylate LIMK1s, the splice variant of LIMK1 lacking kinase activity, which can be phosphorylated on Thr 508 by PAK or ROCK but does not undergo autophosphorylation on serine residues (Arber *et al*, 1998 and unpublished observation). Cell lysates of 293T cells expressing GST-LIMK1s were incubated in the presence of mammalian GST-SSH-t or GST-SSH-t (CS) for 30 min, followed by Western blot analysis with an antibody that recognizes phospho-Thr-508 (Supplementary Figure 1). The level of p-LIMK1 decreased after incubation with SSH-t but not with SSH-t (CS), indicating that SSH can dephosphorylate LIMK1 on Thr 508 (Figure 6A). To test if SSH can dephosphorylate the autophosphorylated serine residues, constitutively active LIMK1-EE508 was immunoprecipitated from HEK293 cells and was autophosphorylated in the *in vitro* kinase assay. The labeled protein was incubated for 1 h with bacterially expressed GST-SSH-t, followed by Western blotting and phosphorImager analysis. In the presence of GST-SSH-t, the levels of p-LIMK1 and p-LIMK-EE508 were reduced by five- and three-fold, respectively (Figure 6B), indicating that SSH can dephosphorylate LIMK1 on autophosphorylation sites.

Next we examined whether the dephosphorylation of LIMK1 by SSH resulted in downregulation of its kinase activity towards cofilin. F-LIMK1, GST-SSH-t, and GST-SSH-t (CS) were expressed separately in 293T cells. The cell lysate of F-LIMK1-transfected cells was incubated for 40 min with glutathione-bound GST-SSH-t, GST-SSH-t (CS) or GST alone.

Figure 4 Purified LIMK1 and hSSH-1L interact directly *in vitro* through the kinase domain of LIMK1 and the N-terminal half of hSSH-1L. (**A**) Silver-stained gel (left) and immunoblots of purified LIMK1 (right) (lane 1) and hSSH-1L (lane 2). In lane 3 the 2.5 M urea wash prior to elution of hSSH-1L was omitted. Note that the SSH-1L and LIMK1 preparations used for *in vitro* binding (lanes 1 and 2) are devoid of both actin and 14-3-3 immunoreactivity. Both showed minor contaminating bands by SDS–PAGE that are probably degradation products. (**B**) Nickel resin and glutathione-Sepharose pulldown assays of purified His-myc hSSH-1L and GST-LIMK1. The His-myc hSSH-1L is pulled down with glutathione beads only in the presence of GST-LIMK1, and the GST-LIMK1 is pulled down on nickel beads only in the presence of His-myc hSSH-1L. (**C**) Immunoblots of pulldown experiments showing direct interaction between bacterially expressed LIMK1 kinase domain (His-kinase) and truncated SSH (GST-SSH-t) proteins.

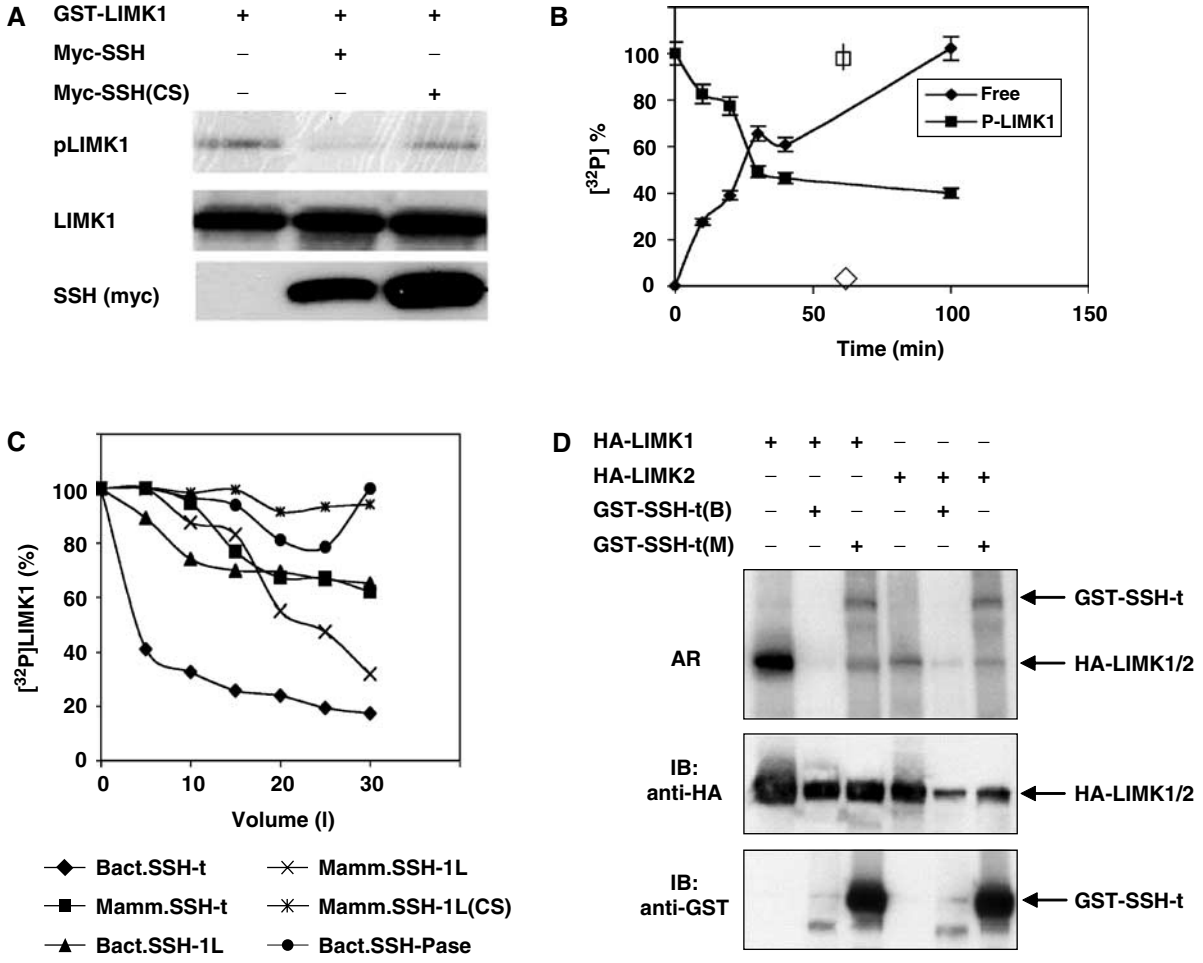

Figure 5 Slingshot is a LIMK1 phosphatase. Active and inactive myc-SSH-1L proteins were immunopurified with anti-myc mAb and GST-LIMK1 was affinity-purified with glutathione Sepharose. The purified proteins were incubated in the presence of 5 μCi [γ^{32}P]ATP for 30 min, followed by Western blotting and autoradiography. (**A**) The level of GST-LIMK1 phosphorylation is greatly decreased only in the presence of active myc-SSH-1L (top panel). The levels of GST-LIMK1 (middle panel) and myc-SSH (bottom panel) were analysed by Western blotting. (**B**) Time course of *in vitro* phosphatase assay with [^{32}P]LIMK1 as substrate. The relative level of phosphorylated LIMK1 was calculated from the ratio of p-LIMK1/LIMK1 values determined by densitometry in the presence of active SSH. The level of [^{32}P] released during the assay was measured and plotted. The level of [^{32}P]LIMK1 after 60 min incubation with myc-SSH-1L (CS) is shown as an open square and the level of [^{32}P] released as an open diamond. (**C**) Comparison of the activities of full-length and C-terminal truncated mammalian and bacterial SSH expressed proteins. Each point was calculated taking into consideration the amounts of protein present in the assay. (**D**) The effect of bacterially and mammalian expressed GST-SSH-t on the phosphorylation of HA-LIMK1 and HA-LIMK2 by *in vitro* kinase assay. Bacterially expressed SSH-t(B) is more active than SSH-t(M) expressed in mammalian cells (top panel). Note that SSH-t expressed in mammalian cells is phosphorylated, probably by a kinase that is present in the protein complex. After phosphorImaging, the filter was probed with anti-HA mAb (middle panel) and with rabbit anti-GST antibodies (bottom panel) to demonstrate the levels of HA-LIMK1&2 and the SSH proteins, respectively.

The supernatant was separated and subjected to immunoprecipitation with anti-Flag beads, followed by the *in vitro* kinase assay in the presence of chicken cofilin. The activity of LIMK1 toward cofilin was reduced five-fold after incubation with GST-SSH-t, but decreased only slightly after incubation with GST-SSH-t (CS) or GST alone (Figure 6C), indicating that dephosphorylation of LIMK1 by SSH results in downregulation of its activity. Similarly, the level of [^{32}P]LIMK1 was also reduced five-fold after incubation with SSH-t, but only slightly after incubation with SSH-t (CS) or GST (Figure 6C), indicating that dephosphorylation of LIMK1 by SSH-t results in downregulation of its activity towards cofilin.

The activity of hSSH-1L is regulated by F-actin and by phosphorylation

His/myc-hSSH-1L is active when expressed in cells, dephosphorylating completely the endogenous pool of ADF/cofilin, whereas the CS mutant is inactive (Supplementary Figure 2). When overexpressed hSSH-1L and its CS mutant were purified on nickel resin, they both bound actin and 14-3-3 in equal amounts (Supplementary Figure 3A). However, only hSSH-1L, but not its CS mutant, was able to dephosphorylate pAC *in vitro* (data not shown; Niwa *et al*, 2002). When the nickel resin containing the bound hSSH-1L was washed free of contaminating proteins with 2.5 M urea before elution, the purified hSSH-1L lost its pADF phosphatase activity, which was restored upon addition of actin (Supplementary Figure 3B). This restoration of activity depended upon the continuous presence of F-actin (Supplementary Figure 3C).

Purified hSSH-1L, as well as 1S, 2S, and 3S, stained positively for phosphate (Figure 7A). Phosphorylation is primarily on serine as shown by 2D phosphoamino-acid analysis of overexpressed GST-SSH-t (Figure 7B). Interestingly, bacterially expressed GST-SSH-t was also pri-

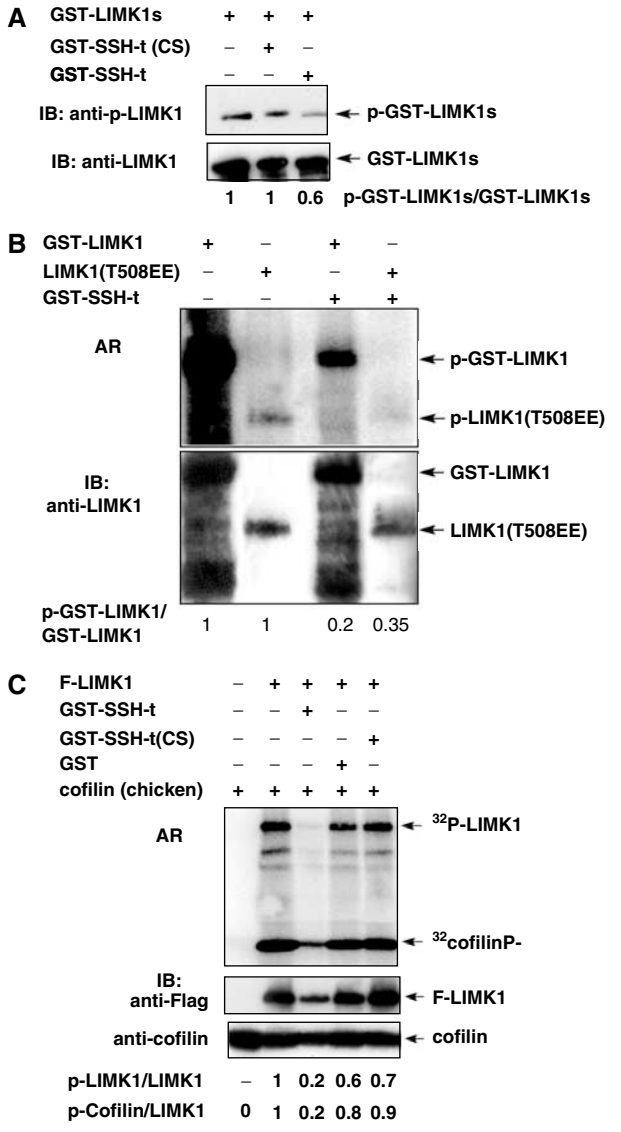

Figure 6 SSH-t downregulates the activity of LIMK1 towards cofilin by dephosphorylating Thr 508 and other phosphorylated serine residues. (**A**) Lysates of GST-LIMK1s expressing 293T cells were subjected to Western blotting before and after incubation with mammalian expressed purified GST-SSH-t or GST-SSH-t (CS). The filter was probed with anti-pLIMK1 antibody, stripped and reprobed with rat anti-LIMK1 mAbs. Incubation with SSH-t, but not with SSH-t (CS), resulted in decreased level of p-LIMK1. The numbers at the bottom represent the ratio between p-GST-LIMK1 and GST-LIMK1 as determined by densitometry. (**B**) Constitutively active LIMK1-EE508 and GST-LIMK1 were immunoprecipitated or pulled down from overexpressing mammalian cells and subjected to *in vitro* kinase assay. In the presence of bacterially expressed GST-SSH-t, the levels of p-LIMK1 and p-LIMK1-EE508 proteins were reduced by five- and three-fold, respectively. (**C**) Lysate of F-LIMK1-expressing cells was incubated with glutathione-bound GST-SSH-t, GST-SSH-t (CS) or GST expressed in mammalian cells. After centrifugation, the supernatants were precipitated with anti-Flag beads followed by *in vitro* phosphatase assay with [^{32}P]cofilin as a substrate. In the presence of GST-SSH-t, the levels of p-cofilin and p-LIMK1 were greatly reduced.

marily phosphorylated on serine by PAK4 *in vitro* (Figure 7B). The majority of the phosphate could be removed from the hSSH-1L isoform by incubation with λ-phosphatase for 1 h (Figure 7A). Even after dephosphorylation, the purified hSSH-1L requires F-actin for activity (Figure 7C). In the presence of F-actin, the dephosphorylated form of hSSH-1L has greater phosphoADF phosphatase activity than the phosphorylated hSSH-1L fraction (Figure 7C and D).

SSH is phosphorylated and inactivated by PAK4

To test if the kinase that phosphorylates hSSH-1L associates with it, GST-SSH-t was pulled down from transfected 293T cells and its phosphorylation analysed after incubation with [γ^{32}P]ATP, followed by Western blotting and autoradiography. The resulting incorporation of [^{32}P] into a band that is recognized by anti-GST antibody to be GST-SSH-t suggests that SSH is phosphorylated by a co-immunoprecipitating kinase (Figure 5D). In contrast, bacterially expressed SSH-t was not phosphorylated (Figure 5D).

As LIMK1 forms a complex with SSH-1L, we tested the possibility that it or one of the protein kinases known to modulate LIMK1 activity (PAK1, PAK4, and ROCK) might phosphorylate SSH-1L. Myc-SSH-1L, expressed in 293T cells, was used as a substrate for active HA-PAK4 (PAK4Δ) in an *in vitro* kinase assay. The level of phosphorylation of myc-SSH-1L was greatly increased in the presence of PAK4 (Figure 7E), suggesting that PAK4 is a SSH-1L kinase. To evaluate the effect of PAK4-mediated phosphorylation of SSH on its phosphatase activity towards LIMK1, [^{32}P]LIMK1 was incubated in the presence of phosphorylated and unphosphorylated SSH-t. LIMK1 phosphorylation was greatly reduced in the presence of unphosphorylated SSH-t; however, in the presence of phosphorylated SSH-t, the level of p-LIMK1 was similar to that of p-LIMK1 alone (Supplementary Figure 4). Furthermore, when phospho-cofilin (p-cofilin) was incubated in the presence of phosphorylated SSH-t, its phosphorylation was not affected, while in the presence of unphosphorylated SSH the level of p-cofilin was greatly reduced, indicating that PAK4 controls the activity of SSH (Figure 7F).

hSSH-1L binds 14-3-3 in a phosphorylation-dependent manner

hSSH-1L co-sediments with F-actin in the presence or absence of 14-3-3 (Figure 8A). However, there is a 28±8% (s.d.) decrease in the amount of hSSH-1L co-sedimenting with F-actin when 14-3-3ζ is preincubated with the hSSH-1L for 10 min prior to addition of F-actin compared to when actin was preincubated with hSSH-1L before adding 14-3-3ζ. Similarly, the amount of 14-3-3ζ co-sedimenting is also reduced by 28±9% (s.d.), suggesting that binding of 14-3-3ζ to the C-terminal region of hSSH-1L affects its ability to bind actin. When hSSH-1L is treated with λ-phosphatase, it loses its ability to bind 14-3-3ζ. This was demonstrated both by GST pulldowns of 14-3-3ζ and by nickel-resin pulldown of His-myc-SSH-1L (Figure 8B). Although the dephosphorylation of hSSH-1L eliminates its binding to 14-3-3ζ (Figure 8B), addition of 14-3-3ζ to the phosphoADF dephosphorylation assay did not reduce the activity of the hSSH-1L in the presence of F-actin (Figure 8C).

To assess the role of hSSH-1L and 14-3-3 on actin reorganization *in vivo*, we overexpressed hSSH-1L (data not shown) or its CS mutant (Figure 9) in Saos-2 cells. Overexpression of hSSH-1L but not the CS mutant caused complete dephosphorylation of AC as measured on Western blots (Supplementary Figure 2). Accompanying this was the formation of abnormal F-actin accumulations within the

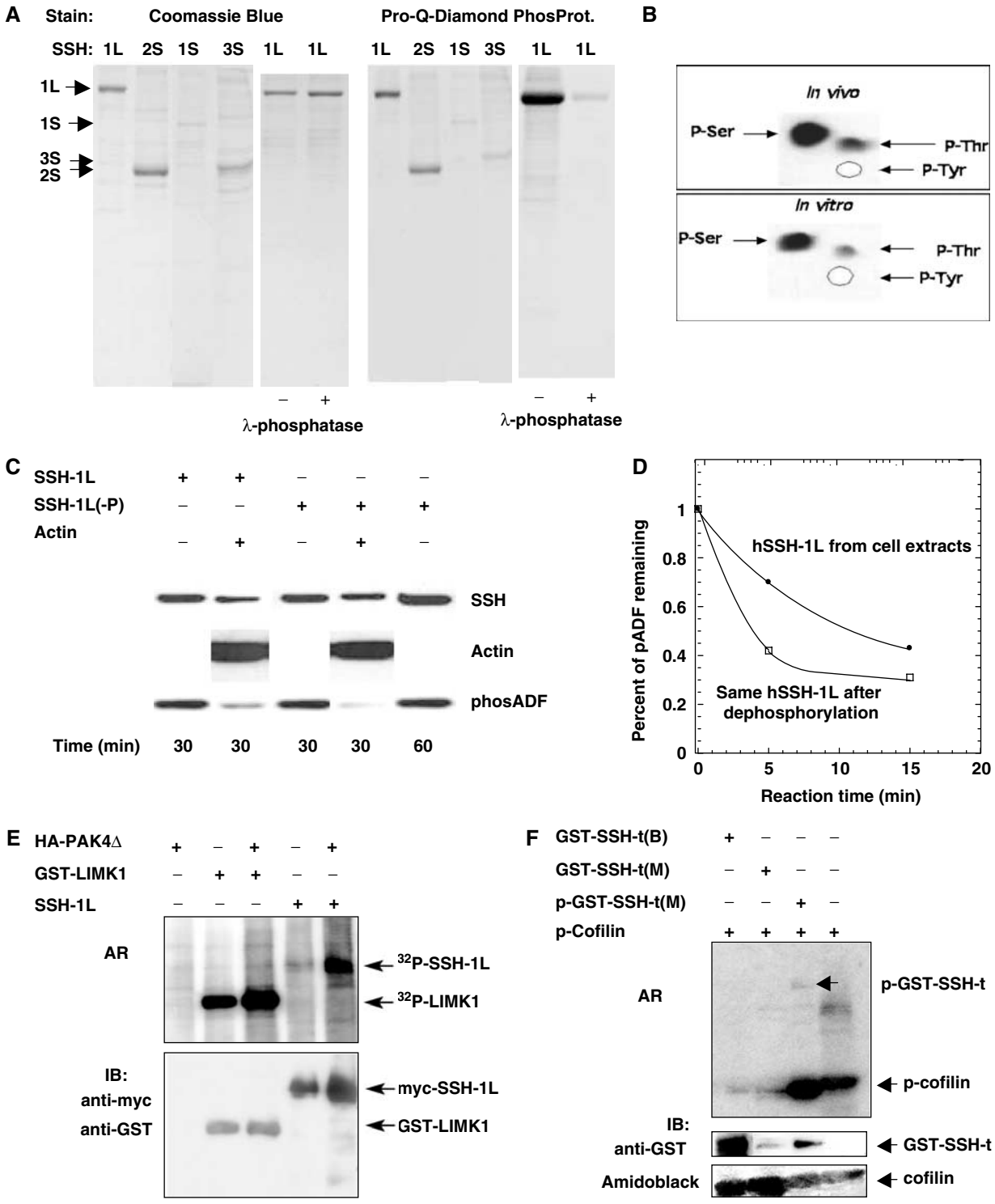

Figure 7 hSSH-1L is a phosphorylated on serine residues and phosphorylation inhibits its activity toward pADF and is necessary for binding 14-3-3ζ. (**A**) Coomassie Blue stained nickel-resin purified hSSH isoforms isolated from overexpressing HEK 293 cells (left panels) are phosphorylated as shown by staining with the Pro-Q Diamond phosphoprotein stain (right two panels). Treatment of hSSH-1L with bacterial λ-phosphatase for 60 min markedly reduced the phosphoprotein staining (far right panel) although the total protein loaded remains constant (Coomassie Blue panel). The images of the phosphoprotein stain have been inverted for easier visualization of the bands. (**B**) Phosphoamino analysis of GST-SSH-t, purified from overexpressing mammalian cells that had been labelled with [^{32}P]orthophosphate (top), and of bacterially expressed GST-SSH-t labelled *in vitro* by PAK4 and [γ^{32}P]ATP (bottom). (**C**) Following λ-phosphatase treatment, hSSH-1L is repurified on nickel resin and is devoid of phosphatase activity (including λ-phosphatase) in the absence of actin (far right lane). In the presence of actin, the mammalian cell derived hSSH-1L is active both before and after dephosphorylation. (**D**) Time course of dephosphorylation of pADF during incubation with hSSH-1L before and after treatment with λ-phosphatase. (**E**) PAK4 is a SSH-1 kinase. PAK4Δ is active as it increases phosphorylation of its known substrate LIMK1 by 1.8-fold. Phosphorylation of SSH-1L by an equal amount of PAK4Δ is even greater. (**F**) SSH-t phosphorylated *in vitro* by PAK4 is unable to dephosphorylate cofilin. [^{32}P]cofilin was greatly reduced by mammalian and bacterially expressed GST-SSH-t, but not when treated with bacterially expressed GST-SSH-t phosphorylated by PAK4Δ (top panel). The level of GST-SSH-t proteins was determined by probing with anti-GST (middle panel) and that of cofilin by staining with amido black.

cytoplasm (Figure 9). The effects of the CS mutant were more pronounced than those induced by wild-type hSSH-1L at identical levels of expression (data not shown). Overexpression of the hSSH-1S did not induce this phenotype, indicating that the actin reorganization was most likely a direct result of the F-actin-binding property of the C-terminal extension of hSSH-1L. Co-expression of the 14-3-3ζ with either the SSH-1L or its CS mutant significantly decreased the number of cells with the strong abnormal phenotype from >30% to <15% (Figure 9B), demonstrating that one major effect of the *in vivo* interaction between SSH-1L and 14-3-3ζ is to regulate the binding of the SSH-1L to F-actin. Taken together, our results suggest that 14-3-3ζ binds to hSSH-1L in a phosphorylation-dependent manner, that its binding to phospho-SSH-1L reduces the ability of the hSSH-1L to bind to F-actin, but that its binding does not alter its pADF phosphatase activity.

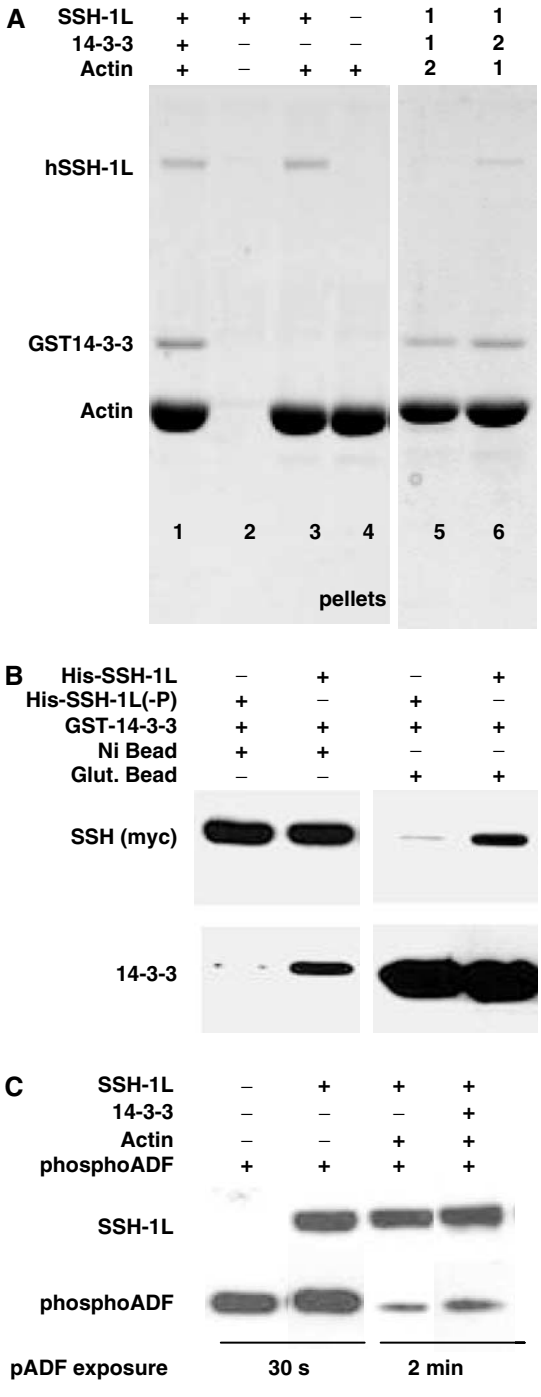

Figure 8 The phosphorylation state of hSSH-1L affects its binding to 14-3-3ζ, but not to F-actin. (**A**) SDS–PAGE analysis of pellets (400 000 $g \times 20$ min) from an F-actin sedimentation (2.5 μM actin and 1.5 μM GST-14-3-3) along with hSSH-1L (single example of triplicates). hSSH-1L sediments only with F-actin (lanes 1 and 3) but not alone (lane 2). Lanes 5–6: numbers above lanes are order of addition. In lane 5, hSSH-1L and 14-3-3ζ were incubated together for 10 min prior to addition of the actin. In lane 6, the actin and hSSH-1L were incubated 10 min before adding 14-3-3ζ. (**B**) Dephosphorylated hSSH-1L does not bind 14-3-3ζ. After dephosphorylation with λ-phosphatase, the repurified His-hSSH-1L was incubated with GST-14-3-3ζ and reciprocal pulldowns were performed with nickel and glutathione resins. Immunoblots of the pulled down proteins were compared with the pull down of hSSH-1L before λ-phosphatase treatment. (**C**) 14-3-3ζ added to hSSH-1L isolated from mammalian cells (phosphorylated form) does not activate its phosphatase activity, nor does it inhibit its activity in the presence of F-actin. All assay time points shown are 15 min incubations. The pADF signal in the right two lanes was not visible at 30 s, so a 2 min exposure is shown. The signal remaining in samples plus and minus 14-3-3ζ is less than 5%.

Discussion

ADF/cofilin family members are important regulators of the actin cytoskeleton as they enhance dynamics of actin filaments. LIMK inactivates AC by phosphorylation of ser 3. Another negative regulator of AC activity is 14-3-3, which binds to pAC (Gohla and Bokoch, 2002). In contrast, SSH phosphatases activate AC by dephosphorylation (Niwa *et al*, 2002).

The activity of LIMK is also regulated by phosphorylation (Edwards *et al*, 1999). The effector kinases of the Rho-GTPases, ROCK and PAK, activate LIMK by phosphorylation of a Thr in the activation loop of the kinase (residue 508 or 505 in LIMK1 and LIMK2, respectively). The activated kinase undergoes autophosphorylation on several serine residues, resulting in increased LIMK activity (Amano *et al*, 2002; Sumi *et al*, 2002 and our unpublished results). Here we demonstrated interaction between LIMK1 and SSH-1L that is mediated via the kinase domain of LIMK1 and the N-terminal domains of hSHH-1L. The A + B domains and the phosphatase domain alone can interact with the kinase domain of LIMK1. It is most likely that this interaction is direct and does not require post-translational modifications because this association takes place also between proteins that are bacterially expressed. Interaction between LIMK1 and SSH-1L resulted in time- and concentration-dependent dephosphorylation of LIMK1, indicating that SSH-1 is both an AC and LIMK1 phosphatase. Surprisingly, the phosphatase activity of SSH-1 towards LIMK1 is greater than towards LIMK2, suggesting that the activity of these two kinases may be regulated differently. We found that SSH-1 dephosphorylates LIMK1 on both Thr 508 and the autophosphorylated serine residues, resulting in inhibition of LIMK1 activity. The finding that SSH-1 is a LIMK1 phosphatase is significant because it demonstrates that SSH-IL can dephosphorylate two different

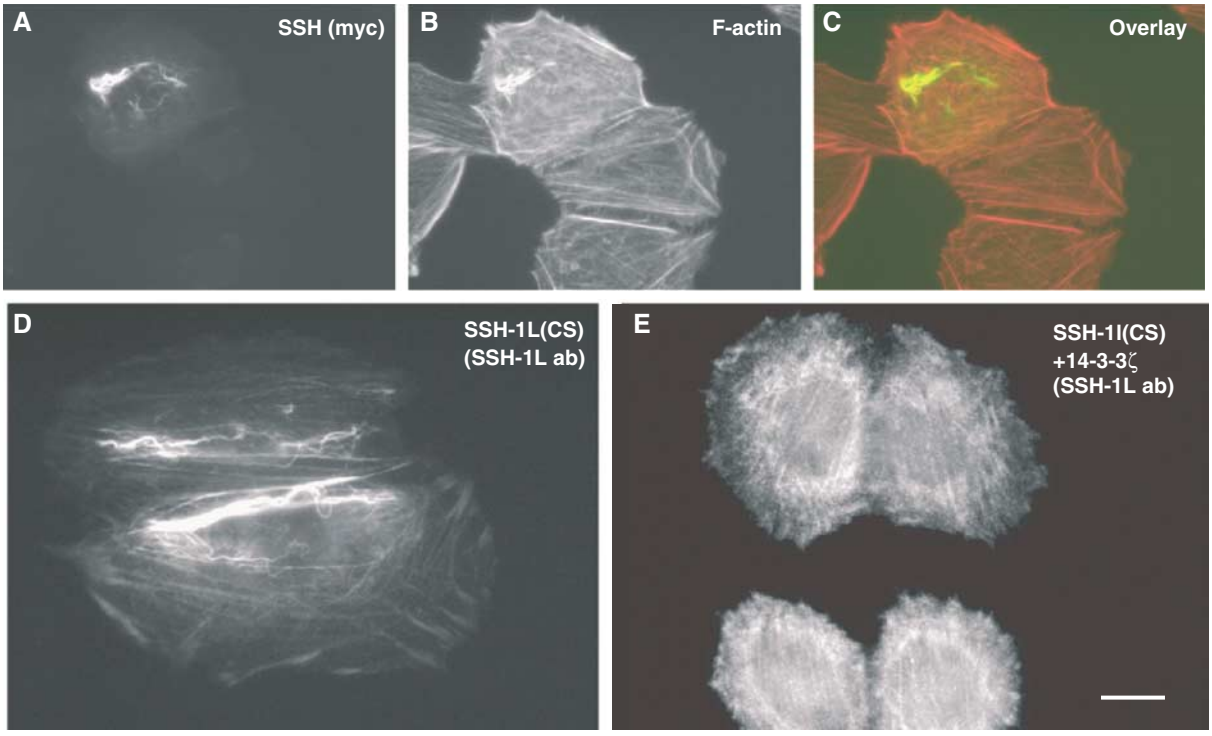

Figure 9 Overexpressed SSH-1L alters cellular F-actin structure in a phosphatase-independent manner and co-expression of 14-3-3ζ inhibits these alterations. Overexpression of myc-SSH-1L (CS) results in abnormal accumulations that co-stain for F-actin and myc (**A–C**) but also for SSH-1L (**D**). Co-expression of SSH-1L (CS) and 14-3-3ζ (**E**) reduces abnormal structures and results in more normal slingshot distribution. Bars = 10 μm.

proteins involved in the same signal transduction pathway, both of which enhance AC activity.

During the revision of this paper, it was demonstrated that actin binding to the C-terminal actin-binding domain of SSH phosphatase greatly increased its activity (Nagata-Ohashi *et al*, 2004), a result we have independently confirmed. As bacterially expressed hSSH-t is catalytically active and does not bind strongly to actin, or require actin for its activity, the role of the C-terminal extension of SSH-1L appears to be autoinhibitory. We propose that F-actin binding to the C-terminal extension of hSSH-1L serves to enhance substrate access to the catalytic domain.

hSSH-1L is phosphorylated principally on serine residues and its activity is negatively regulated by phosphorylation. Although dephosphorylation of purified phospho-SSH-1L did not alter its requirement for F-actin for activation, it did increase its phosphatase activity towards phosphoADF, indicating that SSH-1L activity is downregulated by phosphorylation. In addition, the phosphatase activity of SSH toward LIMK1 and cofilin was inhibited by phosphorylation of hSSH by PAK4. Recently, it was shown that the phosphorylation of two serine residues in the C-terminal actin-binding domain of SSH-1L, S937, and S978 is responsible for the binding of 14-3-3 (Nagata-Ohashi *et al*, 2004). However, we have shown here that PAK4 phosphorylates the truncated form of SSH, lacking the C-terminal 14-3-3 and actin-binding domain. Thus, SSH is tightly regulated by phosphorylation on sites other than S937 and S978.

At least seven isoforms of 14-3-3 proteins are expressed in mammalian cells and most have overlapping binding specificities with their phosphorylated serine-binding partners (Fu *et al*, 2000). These proteins, particularly 14-3-3ζ, bind to pAC and, when overexpressed in cells, protect pAC from dephosphorylation, resulting in increased levels of F-actin in transfected cells (Gohla and Bokoch, 2002). Although 14-3-3 is also a LIMK1-binding protein, the function of this interaction is not yet clear (Gohla and Bokoch, 2002). In this study, we found that 14-3-3ζ binds to phosphorylated hSSH-1L (less-active form), but it does not bind to the more active nonphosphorylated hSSH-1L. The presence of 14-3-3ζ reduces by 28% the binding of hSSH-1L (presumably the phosphorylated species) to F-actin, suggesting that it further inhibits hSSH-1L activity that is initiated by phosphorylation. The 28% decrease in binding probably represents the amount of phosphorylated (inactive) hSSH-1L in the purified fraction from cell extracts, because we observe a similar 25–30% increase in the activity of this same hSSH-1L preparation following dephosphorylation. However, the *in vitro* rate of dephosphorylation of pADF by hSSH-1L is not altered by addition of 14-3-3ζ, nor does 14-3-3ζ activate hSSH-1L in the absence of actin, suggesting that the effects of overexpressed 14-3-3ζ in protecting dephosphorylation of ADF/cofilin *in vivo* are not directly mediated via inhibition of SSH-1L activity.

Overexpression of 14-3-3γ in MCF-7 breast carcinoma cells inhibited neuregulin-induced translocation of the SSH-1L to lamellipodia and prevented dephosphorylation of pAC (Nagata-Ohashi *et al*, 2004). Here we show that the actin-binding properties of SSH-1L are independent of its phosphatase activity and that 14-3-3ζ can reverse the effects of SSH-1L overexpression on actin morphology. Although 14-3-3ζ interacts with the kinase domain of LIMK1, it does not protect it from dephosphorylation by SSH (Supplementary Figure 4).

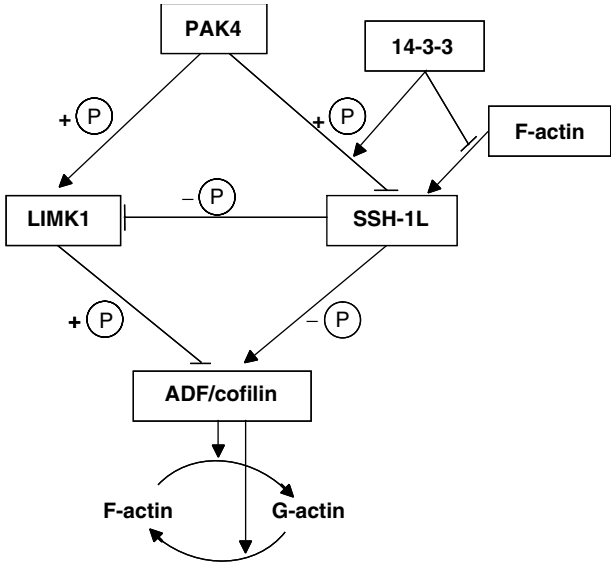

Figure 10 Schematic representation of the regulatory interactions between the new players that regulate the actin cytoskeleton. PAK4 activates LIMK1 and inactivates SSH-1L by phosphorylation. SSH also plays a dual role. It dephosphorylates and inactivates LIMK1 and dephosphorylates and activates ADF/cofilin, resulting in a net increase in ADF/cofilin activity and actin filament turnover. The other players in this pathway are F-actin and 14-3-3ζ. F-actin is necessary for SSH-1L activity and the interaction of pSSH-1L and F-actin is modulated by 14-3-3ζ. Stimulatory (arrows) and inhibitory interactions (blocked lines) are shown.

Taken together, these results suggest that the role of 14-3-3 in binding to phosphorylated hSSH-1L is to further reduce its interaction with F-actin, but that 14-3-3 has no direct effect on the ability of active hSSH-1L to dephosphorylate pAC and LIMK1. Further studies are required to determine if 14-3-3 may also affect the dephosphorylation (activation) of hSSH-1L.

We previously demonstrated that PAK4 interacts with LIMK1 via its LIM domains and that this interaction results in LIMK1 activation and increased AC phosphorylation (Dan *et al*, 2001). The importance of phosphorylation for down-regulating SSH activity is demonstrated here and one of the enzymes responsible for its phosphorylation is identified as PAK4. Thus, PAK4, which when expressed *in vivo* affects F-actin dynamics at least in part through increasing the pool of pAC, activates LIMK1 and inactivates SSH-1L.

In conclusion, the interactions between several players in the regulation of ADF/cofilin, and thus regulation of the actin cytoskeleton, have been identified here (Figure 10). PAK4 is a pivotal player in this pathway by acting as a dual regulator to activate LIMK1 and inactivate SSH-1L, whereas F-actin serves to activate SSH-1L, which inactivates LIMK1. The interaction of phospho-SSH-1L and F-actin is modulated by 14-3-3ζ, which may play more complex roles that require further study.

Materials and methods

Plasmid constructs and adenoviruses

Myc-Rac1V12 in pcEXV-3 was generously provided by Alan Hall (London, UK). hSSH-1L, hSSH-1S, hSSH-2S, hSSH-3S and hSSH (C393S) cDNAs in pcDNA3.1/Myc-His(+) vector were generously provided by Tadashi Uemura (Kyoto, Japan). Adenoviruses expressing the various SSH constructs were prepared by subcloning SSH-1L, -1L(C393S), -1S, and -3S *Hind*III to *Pme*I or SSH-2S *Kpn*I to *Pme*I from pcDNA3.1/Myc-His(+) into pAdTrack *Hind*III or *Kpn*I to EcoRV. 14-3-3ζ Adenovirus was prepared by subcloning a *Bam*HI to *Not*I fragment from pcDNA3, provided by Gary Bokoch (La Jolla, CA), into *Bgl*II to *Not*I in pAdTrack. Virus was produced as described previously (Minamide *et al*, 2003).

The C-terminal hSSH-1L deletion constructs (SSH-t) were generated by subcloning a 1.6 kb *Bam*H1 fragment into the *Bam*H1 site of pGEX-4T and pEGB vectors. The A+B domains construct was generated by subcloning a 1 kb *Bam*H1/*Dra*1 5′ fragment into the *Bam*H1/*Sma*1 site of pGEX-4T and the phosphatase domain (aa 338–533) was cloned into the *Bam*H1 site of pGEX-4T by PCR. The full-length and truncated Flag- and GFP-LIMK1 cDNAs and the GST-LIMK1 construct were described previously (Foletta *et al*, 2003). To generate His-tagged LIMK1 kinase domain construct, a 1.26 kb *Xho*I fragment was cloned into the *Xho*I site of the bacterial expression vector pET-15b (Novogen). HA-PAK4 delta construct was previously described (Dan *et al*, 2001).

In vivo [^{32}P] labelling of phosphoproteins

Myc-SSH-1L constructs were electroporated into COS-7 cells. After 48 h the cellular phosphoproteins were labelled *in vivo* with 1 mCi/ml [^{32}P]orthophosphate for 6 h. Myc-SSH-1L was immunoprecipitated with 5 μg anti-myc mAb (Clone 9E10, Zymed). The immune complexes were separated on a 10% Tris–Glycine pre-cast gel (Invitrogen, Novex), transferred onto Hybond-C nitrocellulose membrane (Amersham) and subjected to either autoradiography or phosphorImaging.

SDS–PAGE

Protein samples were boiled in SDS-gel sample preparation buffer (Laemmli, 1970). Protein concentrations were determined using either the Bio-Rad reagent (Bio-Rad Catalog 500-0006) or the filter paper dye-binding assay (Minamide and Bamburg, 1990). Samples were separated by electrophoresis on mini-protean units (Bio-Rad) using isocratic polyacrylamide gels (7–15%, depending on the size of the proteins being separated).

Transfections, immunoprecipitation and immunoblotting analysis

cDNA constructs were electroporated into COS-7 cells or transfected into Saos-2, HEK293 or 293T cells by FuGENE 6 (Roche Diagnostics) or Lipofectamine (InVitrogen). After 48 h, cells were lysed in PBS lysis buffer containing 50 mM Tris–HCl (pH 7.4), 150 mM NaCl, 1% Triton X-100, protease inhibitor cocktail (Roche Cat. # 1 836 153), 10 mM NaF, 1 mM Na_3VO_4, and 10 mM NaP_2O_7 and sonicated for 10 s. Target proteins were either affinity purified with glutathione Sepharose or 30 μl of Flag M2 beads (Sigma) or immunoprecipitated with 2 μl of rabbit anti-myc antibodies (1:1000; Santa Cruz) as described in Foletta *et al* (2003). Endogenous LIMK1 was immunoprecipitated with 2 μl of mouse anti-LIMK1mAb (BD Transduction Laboratories, Clone 42). Immunoblots were probed with the following antibodies: rabbit polyclonal Abs: anti-myc (1:1000; Santa Cruz), anti-GFP (1:5000; Santa Cruz), anti-14-3-3 (pan) (1:1000; Santa Cruz), anti-14-3-3ζ (1:1000; Santa Cruz), anti-Flag (1:3000; Sigma), anti-GST (1:3000; Molecular Probes); mouse mAbs: anti-myc (1:3000; Cell Signaling), 1.0 ng/μl anti-c-myc (Clone 9E10, Zymed), anti-HA.11 (1:3000; ascites fluid of clone 16B12, Babco), anti-actin C4 (1:2500; ascites fluid, ICN Cat # 691001) or anti-Flag M2 (10 ng/μl; Sigma). Rat anti-LIMK1 mAb (Foletta *et al*, 2004) at 0.2 ng/μl and affinity-purified rabbit anti-phosphoADF/cofilin Abs (Meberg *et al*, 1998) at 0.5 ng/μl were used on Western blots. Appropriate alkaline phosphatase or horseradish peroxidase-conjugated secondary antibodies were used at their recommended dilutions and were followed with chemiluminescent substrates (ECL, Amersham; Supersignal West Pico or Supersignal West Extended Duration Substrate, Pierce Biotech.) and CL-XPosure™ film (Pierce Biotech.) to detect the chemiluminescence.

Purification of His-myc hSSH-1L and GST-LIMK1

HEK 293 cells infected with adenovirus expressing 6xHis/myc-tagged hSSH-1L were lysed by sonication in 50 mM Tris, pH 7.5, containing 150 mM NaCl, 10 mM NaF, 10 mM imidazole, 2 mM DTT, and protease inhibitor cocktail (Morgan *et al*, 1993), and cleared by

centrifugation at 12 500 *g* for 12 min. Lysates were passed over nickel agarose (Ni-NTA-agarose; Qiagen, Hilden, Germany), washed 3 × with lysis buffer containing 20 mM imidazole and 2.5 M urea, and bound material eluted with lysis buffer containing 250 mM imidazole. Eluates were then dialysed in buffer containing 50 mM Tris, pH 7.5, 150 mM NaCl and 2 mM DTT. LIMK1 was isolated by sonicating HEK293 cells transfected with DNA encoding GST-LIMK1 in 50 mM Tris, pH 8.0, containing 100 mM NaCl, 10% glycerol, protease inhibitor cocktail, 2 mM DTT, and 0.2% IGEPAL. Lysates were passed over GST-Sepharose and washed 3 × with 50 mM HEPES, pH 7.4, 150 mM NaCl, 5 mM $MgCl_2$, 2 mM $MnCl_2$, and 2 mM DTT. Bound material was eluted with wash buffer containing 10 mM glutathione, or the washed beads were used directly to generate phosphoADF used in the SSH pADF phosphatase assays.

In vitro kinase assay

This assay was performed as described by Foletta *et al* (2003).

Protein phosphatase assays for SSH activity

In vitro assays with phosphoADF as substrate. Chick brain ADF (Giuliano *et al*, 1988) was phosphorylated *in vitro* for 2 h at room temperature with solid phase GST-LIMK1 purified as described above. SSH activity was assessed by incubating at 30°C 40 µl of SSH with 400 ng of phosphorylated chick brain ADF, removing 10 µl aliquots at various intervals, boiling with SDS sample preparation buffer and immunoblotting with anti-phosphoADF antibody (Meberg *et al*, 1998). The reaction buffer contains 50 mM HEPES, pH 7.4, 120 mM NaCl, 2.0 mM $MgCl_2$, 1.0 mM $MnCl_2$, and 1.0 mM DTT.

Assays in cell lysates with p-LIMK1 as substrate. Transfected cells in lysis buffer were sonicated for 10 s. Target proteins were either pulled down by glutathione Sepharose or immunoprecipitated with mouse anti-myc mAbs (clone 9E10, Zymed). Phosphatase assays were carried out at 37°C using 5 µl of *in vitro* labelled [^{32}P]GST-LIMK1 as substrate. The phosphatase assay was performed at various times in assay buffer containing 30 mM Tris–HCl, pH 7.4, 30 mM KCl, 1 mM EDTA, 0.1 mg/ml BSA, and 20 µl of myc-SSH-1L or the inactive myc-SSH-1L (CS) as immune complex or GST-SSH bound to glutathione Sepharose. Reactions were initiated by addition of [^{32}P]LIMK1 substrate. After centrifugation at 13 000 r.p.m. for 1 min, the radioactivity in the supernatant was quantified. The beads were washed three times in assay buffer and bound proteins were subjected to Western blotting. The level of [^{32}P]LIMK1 was quantified with a PhosphorImager. The level of LIMK1 and SSH was determined by immunoblotting and densitometry.

Cell culture and immunostaining

E18 rat hippocampal neurons (Meberg and Miller, 2003) or Saos-2 cells (Wiggan *et al*, 2002) were cultured as described previously, and fixed in 4% paraformaldehyde/PBS or a cytoskeletal preservation buffer (4% formaldehyde, 10 mM morpholinoethane sulphonate, pH 6.1, 138 mM KCl, 3 mM $MgCl_2$, 2 mM EGTA, 0.32 M sucrose). Cells were blocked and permeabilized in 3% goat serum, 1% BSA, and 0.1% Triton X-100. LIMK1 was detected with 10 µg/ml of rat anti-LIMK1 mAb for 1 h at RT. SSH-1L was detected with 5 µg/ml of affinity-purified rabbit anti-hSSH-1L, 14-3-3 with mouse anti-pan-14-3-3 mAb (Santa Cruz), and F-actin with Alexa-phalloidin (Molecular Probes). Images were acquired using inverted Nikon Diaphot epifluorescence microscopes equipped with Roper Coolsnap or CoolsnapES digital cameras and Metamorph image software (Universal Imaging Corp, West Chester, PA).

Supplementary data

Supplementary data are available at *The EMBO Journal* Online.

Acknowledgements

We thank Dr Tadashi Uemura, Kyoto University, Japan for the generous gifts of slingshot expression vectors, Dr Gary Bokoch, Scripps Research Institute, San Diego for the 14-3-3ζ expression Vector, Dr Alan Hall, UCL, London, UK for the V12rac expression vector, and Alisa Shaw for preparing, amplifying, and titrating of some adenoviruses used here. This work was supported in part by NIH grants GM35126 and NS40371 and Alzheimer's Association grant IIRG-01-2730 to JRB, Christopher Reeve Paralysis Foundation grant SB2-0110-2 to PDS, Canadian Institutes of Health Research grant to OW, Association for International Cancer Research and US Army Medical Research and Material Command (BS), and the Australian NHMRC to OB.

References

Amano T, Kaji N, Ohashi K, Mizuno K (2002) Mitosis-specific activation of LIM motif-containing protein kinase and roles of cofilin phosphorylation and dephosphorylation in mitosis. *J Biol Chem* **277:** 22093–22102

Arber S, Barbayannis FA, Hanser H, Schneider C, Stanyon CA, Bernard O, Caroni P (1998) Regulation of actin dynamics through phosphorylation of cofilin by LIM-kinase. *Nature* **393:** 805–809

Bamburg JR, Wiggan OP (2002) ADF/cofilin and actin dynamics in disease. *Trends Cell Biol* **12:** 598–605

Birkenfeld J, Betz H, Roth D (2003) Identification of cofilin and LIM-domain-containing protein kinase 1 as novel interaction partners of 14-3-3 zeta. *Biochem J* **369:** 45–54

Dan C, Kelly A, Bernard O, Minden A (2001) Cytoskeletal changes regulated by the PAK4 serine/threonine kinase are mediated by LIM kinase 1 and cofilin. *J Biol Chem* **276:** 32115–32121

Edwards DC, Gill GN (1999) Structural features of LIM kinase that control effects on the actin cytoskeleton. *J Biol Chem* **274:** 11352–11361

Edwards DC, Sanders LC, Bokoch GM, Gill GN (1999) Activation of LIM-kinase by Pak1 couples Rac/Cdc42 GTPase signalling to actin cytoskeletal dynamics. *Nat Cell Biol* **1:** 253–259

Foletta VC, Lim MA, Soosairajah J, Kelly AP, Stanley EG, Shannon M, He W, Das S, Massague J, Bernard O (2003) Direct signaling by the BMP type II receptor via the cytoskeletal regulator LIMK1. *J Cell Biol* **162:** 1089–1098

Foletta VC, Moussi N, Sarmiere PD, Bamburg JR, Bernard O (2004) LIM kinase 1, a key regulator of actin dynamics, is widely expressed in embryonic and adult tissues. *Exp Cell Res* **294:** 392–405

Fu H, Subramanian RR, Masters SC (2000) 14-3-3 proteins: structure, function, and regulation. *Annu Rev Pharmacol Toxicol* **40:** 617–647

Giuliano KA, Khatib FA, Hayden SM, Daoud EW, Adams ME, Amorese DA, Bernstein BW, Bamburg JR (1988) Properties of purified actin depolymerizing factor (ADF) from chick brain. *Biochemistry* **27:** 8931–8938

Gohla A, Bokoch GM (2002) 14-3-3 regulates actin dynamics by stabilizing phosphorylated cofilin. *Curr Biol* **12:** 1704–1710

Ikebe C, Ohashi K, Fujimori T, Bernard O, Noda T, Robertson EJ, Mizuno K (1997) Mouse LIM kinase 2 gene: cDNA cloning, genomic organization, and tissue specific expression of two alternatively initiated transcripts. *Genomics* **46:** 504–508

Laemmli UK (1970) Cleavage of structural proteins during the assembly of the head of bacteriophage T4. *Nature* **227:** 680–684

Maekawa M, Ishizaki T, Boku S, Watanabe N, Fujita A, Iwamatsu A, Obinata T, Ohashi K, Mizuno K, Narumiya S (1999) Signaling from Rho to the actin cytoskeleton through protein kinases ROCK and LIM-kinase. *Science* **285:** 895–898

Meberg PJ, Miller MW (2003) Culturing hippocampal and cortical neurons. *Methods Cell Biol* **71:** 111–127

Meberg PJ, Ono S, Minamide LS, Takahashi M, Bamburg JR (1998) Actin depolymerizing factor and cofilin phosphorylation dynamics: response to signals that regulate neurite extension. *Cell Motil Cytoskelet* **39:** 172–190

Minamide LS, Bamburg JR (1990) A filter paper dye-binding assay for quantitative determination of protein without interference from reducing agents or detergents. *Anal Biochem* **190:** 66–70

Minamide LS, Shaw AE, Sarmiere PD, Wiggan O, Maloney MT, Bernstein BW, Sneider JM, Gonzalez JA, Bamburg JR (2003)

Production and use of replication-deficient adenovirus for transgene expression in neurons. *Methods Cell Biol* **71:** 387–416

Morgan TE, Lockerbie RO, Minamide LS, Browning MD, Bamburg JR (1993) Isolation and characterization of a regulated form of actin depolymerizing factor. *J Cell Biol* **122:** 623–633

Nagata-Ohashi K, Ohta Y, Goto K, Mori R, Nishita M, Ohashi K, Kousaka K, Iwamatsu A, Niwa R, Uemura T, Mizuno K (2004) A pathway of neuregulin-induced activation of cofilin-phosphatase Slingshot and cofilin in lamellipodia. *J Cell Biol* **165:** 465–471

Niwa R, Nagata-Ohashi K, Takeichi M, Mizuno K, Uemura T (2002) Control of actin reorganization by Slingshot, a family of phosphatases that dephosphorylate ADF/cofilin. *Cell* **108:** 233–246

Ohashi K, Nagata K, Maekawa M, Ishizaki T, Narumiya S, Mizuno K (2000) Rho-associated kinase ROCK activates LIM-kinase 1 by phosphorylation at threonine 508 within the activation loop. *J Biol Chem* **275:** 3577–3582

Ohta Y, Kousaka K, Nagata-Ohashi K, Ohashi K, Muramoto A, Shima Y, Niwa R, Uemura T, Mizuno K (2003) Differential activities, subcellular distribution and tissue expression patterns of three members of Slingshot family phosphatases that dephosphorylate cofilin. *Genes Cells* **8:** 811–824

Pollard TD, Borisy GG (2003) Cellular motility driven by assembly and disassembly of actin filaments. *Cell* **112:** 453–465

Sumi T, Matsumoto K, Nakamura T (2001) Specific activation of LIM kinase 2 via phosphorylation of thr 505 by ROCK, a rho-dependent protein kinase. *J Biol Chem* **276:** 670–676

Sumi T, Matsumoto K, Nakamura T (2002) Mitosis-dependent phosphorylation and activation of LIM-kinase 1. *Biochem Biophys Res Commun* **290:** 1315–1320

Wiggan O, Fadel MP, Hamel PA (2002) Pax3 induces cell aggregation and regulates mesenchymal–epithelial interconversion. *J Cell Sci* **115:** 517–529

Yang N, Higuchi O, Ohashi K, Nagata K, Wada A, Kangawa K, Nishida E, Mizuno K (1998) Cofilin phosphorylation by LIM-kinase 1 and its role in Rac-mediated actin reorganization. *Nature* **393:** 809–812

